

# Direct imaging of SiO<sub>2</sub> thickness variation on Si using modified atomic force microscope\*

K. M. Mang

*Department of Electronic Engineering, Seoul National University, Seoul, Korea*

Y. Khang

*Department of Physics, Seoul National University, Seoul, Korea*

Y. J. Park

*Department of Electronic Engineering, Seoul National University, Seoul, Korea*

Young Kuk

*Department of Physics, Seoul National University, Seoul, Korea*

S. M. Lee

*Department of Physics, Princeton University, Princeton, New Jersey*

C. C. Williams

*Department of Physics, University of Utah, Salt Lake City, Utah*

(Received 24 July 1995; accepted 16 December 1995)

Thickness of silicon dioxide was measured by combined atomic force microscopy and nanoscopic  $C-V$  spectroscopy. The spatial variation of the oxide thickness and dopant profile on the masked Si were directly imaged. The nanoscopic  $C-V$  reveals the same trends as the macroscopic  $C-V$ . Shadowing effect of phosphorous ions during implantation was observed from dopant profile in masked Si substrates. © 1996 American Vacuum Society.

## I. INTRODUCTION

Fabrication techniques of metal-oxide-semiconductor (MOS) transistors have been improved very rapidly during the last several decades. With this trend, scaling down of MOS transistors is necessary to improve the speed of circuits and the packing density of discrete devices. Both lateral and vertical dimensions of unit devices are reduced to ascertain better electrical characteristics of devices. However, many problems, which have not been noticed in the process of fabrication of large scale devices, cause adverse effects in operation of the scaled-down device. The reliability of the dielectric layer, silicon dioxide in the case of MOS transistors, becomes an increasingly crucial factor in the design of very large scale integrated (VLSI) circuits with reduced dimensions.

Nowadays, the thickness of oxide layer is decreased to less than 80 Å and is expected to reach 40 Å. In this thickness regime the electrical characteristics of the oxide layer are important as an insulator. Therefore, it is crucial to obtain an oxide layer with uniform thickness and fewer defects. When the thickness of oxide layer is about 40 Å, a small variation of the oxide thickness causes a significant change of the oxide capacitance. With the variation of oxide thickness, discrete devices in one wafer may have different threshold voltages, and symmetry characteristics between discrete devices can be broken. This asymmetry of device characteristics can result in problems in low-voltage operating circuits. In fact, most of the reliability tests performed until now have focused on the generation of interface states

at the silicon-silicon-dioxide interface and charge trapping phenomena in the silicon dioxide layer which influence the electrical characteristics of the MOS structure. Since the variation of the oxide layer thickness in a device may vary the localized electrical characteristics of the device, it is as important as the defect properties of oxide layer.

## II. EXPERIMENT

Scanning capacitance microscopy (SCM) has been refined to measure a 2D dopant profile with a resolution better than 100 nm.<sup>1-3</sup> In order to interpret the data properly, a slight modification to 1D theory is needed to interpret 2D dopant profile measured by SCM. We have utilized SCM to directly measure the spatial variation of oxide thickness with a sub-micron resolution. To obtain the oxide thickness one may use the value of oxide capacitance per unit area.<sup>4</sup> The spatially varying capacitance of the oxide can be determined by the dielectric constant and the thickness of silicon dioxide. Therefore, if one has the information about the oxide capacitance with nanometer resolution, he can obtain the spatial variation of the oxide thickness. We have used an atomic force microscope (AFM) in the repulsive mode for this study. The operation principle of AFM is well known but, briefly, the sample surface is imaged while maintaining constant the force between tip in the AFM cantilever and sample surface ( $10^{-8}$ – $10^{-10}$  N). In order to measure the nanoscopic  $C-V$  characteristics one should make a small metal area as the gate electrode. Because it is difficult to make such a small metal area which determines the spatial resolution with conventional methods, we use a metal-coated AFM tip as the metal gate electrode. By this method we were able to obtain

\*Published without author corrections.

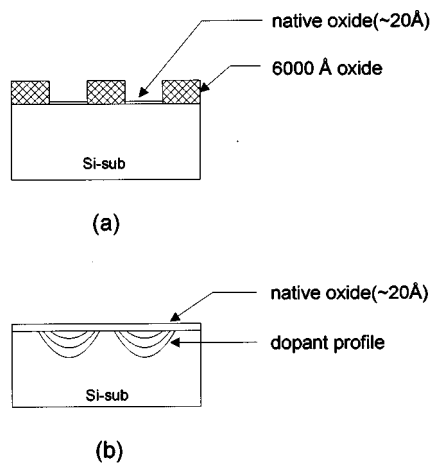


FIG. 1. Cross section of fabricated samples. (a) Sample used to measure the thickness of silicon dioxide. It had periodic patches of silicon dioxide with 6000 Å height on surface. (b) Sample used to measure the dopant profiles. Silicon dioxide was etched and it had a nearly flat native oxide layer over the surface. Solid line in silicon substrate describes expected constant dopant density levels.

the one point  $C-V$  characteristic as well as the spatial variation of the oxide capacitance. For this experiment we have used the contact-mode AFM where the force is measured by optical deflection method<sup>5,6</sup> in air. It is known that adsorbed water molecules sometimes alter the contact force in AFM and become a channel for ionic carriers. This phenomenon was minimized by doing this experiment under dry N<sub>2</sub>, but an UHV AFM is better suited for this. In our contact-mode AFM injected light is divided into two directions with a half-mirror, and the laser beam is detected with a position-sensitive photodetector (PSPD) and also viewed by a charge-coupled device (CCD) camera which makes coarse imaging and zooming of the surface possible. The spatial variation of capacitance is measured by a RCA capacitance sensor<sup>7</sup> in which a resonating circuit with an ultrahigh frequency (UHF) oscillator (915 MHz) and a peak detector are used.<sup>8</sup> The resonant circuit is perturbed by the effect of extra capacitance (capacitance between the AFM tip and sample), although the resonant frequency of the circuit is largely determined by the total stray capacitance of the sensor (~0.1 pF). This extra capacitance may shift the resonant frequency of the sensor and then changes the amplitude of the UHF signal. If the change of capacitance is very small, the output voltage of the peak detector changes linearly with the extra capacitance. A voltage signal mixed with a low-frequency dither (3–10 kHz) is applied to get better signal-to-noise ratio and the output signal of the capacitance sensor is sent to a lock-in amplifier for the phase sensitive detection.

Three samples were used in this experiment. For one point  $C-V$  characteristic,  $p$ -doped Si(100) with 15–20 Ω cm resistivity was used. Silicon dioxide with a thickness of  $42 \pm 1$  Å (measured by ellipsometer) was grown by thermal oxidation in a furnace. In order to image the spatial variation of silicon-dioxide thickness, an artificial mesa structure was fabricated (Fig. 1). First, the same silicon wafer as used in

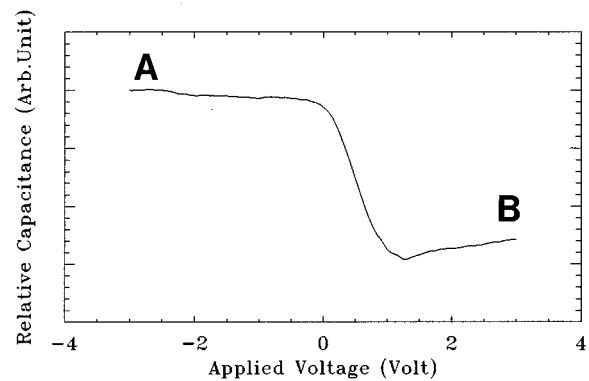


FIG. 2. A one point  $C-V$  characteristic of  $42 \pm 1$  Å (measured by ellipsometer) SiO<sub>2</sub> layer on a  $p$ -doped Si(100) sample.

one point measurement was initially oxidized up to 6000 Å by wet oxidation. The mesa structure was developed by a conventional patterning process. After the patterning, the wafer was implanted with 40 keV phosphorous ions with a dose of  $2 \times 10^{13}$  ion/cm<sup>2</sup>, then annealed at 900 °C for 30 min in N<sub>2</sub> ambient condition. The 6000 Å mesa pattern worked as the mask for the implantation, therefore P was implanted where the oxide was not covered. For the image of dopant density dependent capacitance, the masking oxide was removed by HF, resulting in a flat AFM topography with patterned dopant profile in capacitance measurement as shown in Fig. 1. A conductive cantilever is needed to measure the  $C-V$  characteristics. We modified a commercial silicon cantilever (Nano Probe)<sup>9</sup> by depositing Ni on the cantilever and forming a nickel silicide layer by reacting it.

Since the radius of metal dot used in conventional  $C-V$  measurement is several hundred micrometers, the measured capacitance reflects the averaged value over the large metal dot. However, in present experimental setup the estimated tip radius was  $\leq 100$  nm at best, so were the effective contact area and capacitance resolution. Therefore, one can measure the  $C-V$  characteristic with the spatial resolution of tens of nanometers. Also, we can obtain the spatial information of the capacitance characteristic at a constant dc bias voltage using the scanning capability of AFM.

Figure 2 shows a one point  $C-V$  characteristic on a SiO<sub>2</sub> layer of  $42 \pm 1$  Å (measured by ellipsometer) grown on a  $p$ -doped Si(100) sample. Nearly the same trend in macroscopic  $C-V$  characteristic can be seen in the figure. In a MOS system, the high-frequency  $C-V$  characteristic has two distinct modes (Fig. 2). For this case ( $p$ -type substrate), when the tip bias voltage is negative holes are accumulated at the Si–SiO<sub>2</sub> interface. In this accumulation mode, since the response of the majority carriers to the ac tip voltage is fast enough at the silicon–silicon-dioxide interface, the carrier can follow the variation of the ac tip voltage. Therefore, the measured capacitance reflects only the oxide capacitance which is a function of oxide thickness (A region in Fig. 2). The inversion mode occurs for a positive tip voltage. In this case the Si–SiO<sub>2</sub> interface is inverted with electrons and a

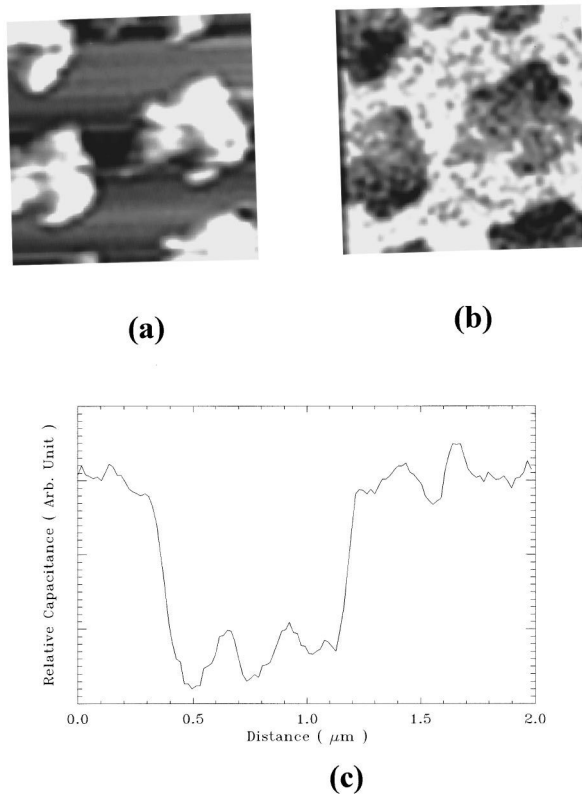


FIG. 3. The topographic image of the mesa structure and the image of oxide capacitance. These  $3.5 \times 3.5 \mu\text{m}^2$  images were obtained with the tip voltage of  $-2 \text{ V}$ . (a) Topographic image. (b) The image of oxide capacitance. The step in this image reflects the sudden change of the oxide thickness as the surface is scanned by the AFM tip: Since the height of the oxide patch is  $6000 \text{ \AA}$ , the measured capacitance on top of the patch is  $1/300$  times of that measured on the native oxide. (c) The cross section of imaged oxide capacitance.

depletion region is formed in the silicon substrate. The measured capacitance for the inversion mode is a serial combination of the oxide capacitance and the silicon capacitance from the depletion layer (B region in Fig. 2). Since the width of depletion layer is a function of the dopant density, the level of measured capacitance for positive tip voltages is determined by the dopant density if the fluctuation of the oxide thickness is negligible, as reported earlier.<sup>1,2,10</sup>

### III. DISCUSSION

In a 1D model, the relation of oxide capacitance and oxide thickness is  $C = \epsilon_{\text{OX}}(A/T_{\text{OX}})$ , when  $A$  is effective area,  $T_{\text{OX}}$  oxide thickness and  $\epsilon_{\text{OX}}$  the dielectric constant of oxide, respectively. Because the tip has three-dimensional structure, the measured capacitance value should be affected by a 3D effect. The modified 1D model, i.e., quasi-1D model, was previously described, showing good agreement with experimental data.<sup>10</sup> Assuming that the dielectric constant of SiO<sub>2</sub> and the resolution of SCM are fixed, the oxide capacitance is only inversely proportional to the thickness of oxide layer. Therefore, the spatial variation of oxide thickness can be directly obtained from the scanning capacitance microscope image while the AFM image reveals the surface topography.

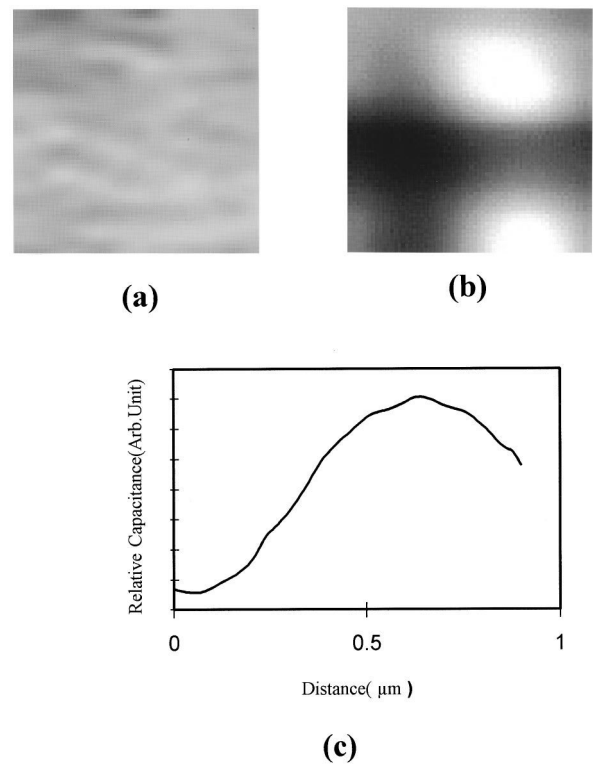


FIG. 4. (a) The topographic and (b) capacitance images of the sample size of  $2.5 \times 2.5 \mu\text{m}^2$ . The 2D dopant profile is imaged due to selectively implanted phosphorous. (c) The cross section of imaged doping dependent capacitance.

If the changes of oxide thickness are very small, the measured SCM image for inversion mode will reflect the change of dopant density. In order to obtain the oxide capacitance image of SiO<sub>2</sub>, a sample with square oxide patches in a checkerboard pattern was prepared. Where bare Si is exposed, native oxide ( $\sim 20 \text{ \AA}$ ) was grown by leaving the sample in air for several days. By scanning the surface, AFM and SCM images were obtained at a constant dc bias voltage. Figures 3(a) and 3(b) show the topographic image of the mesa structure and the image of the oxide capacitance. Also, the cross-section profiles of oxide capacitance image are shown in Fig. 3(c). This  $3.5 \times 3.5 \mu\text{m}^2$  image was obtained with the dc bias voltage of  $-2 \text{ V}$ . The step in topographic reflects the sudden change of the oxide thickness as the surface is scanned by the AFM tip: Since the height of the oxide patch is  $6000 \text{ \AA}$ , the measured capacitance on top of the patch is  $1/300$  times of that measured on the native oxide. The expected variations were obtained since surface corrugation was originated from inversely proportional dependence of the oxide capacitance on the thickness. However, some correction is needed for the absolute calibration of the thickness due to stray capacitance.

In order to measure the 2D dopant profile, phosphorous was implanted on the sample as shown in Fig. 1. The oxide patches work as the mask for the implantation. Since the height of the mask is  $6000 \text{ \AA}$ , comparable to lateral dimension, the shadowing effect will deform the shape of the implanted area. At present it is difficult to measure the 2D

dopant density profile around the edge of the mask by secondary-ion-mass spectrometry with a nanometer resolution; however, this profile can be measured by SCM in inversion mode. To measure only the silicon capacitance originated from the depletion layer, the mesa structure of oxide was etched by HF. After etching the oxide structure, the sample was kept in air for a day to grow a native oxide layer. The topographic and capacitance images with positive tip voltage (+2 V) were obtained simultaneously. Figure 4(a) shows a nearly flat  $2.5 \times 2.5 \mu\text{m}^2$  AFM image, but in the SCM image, the 2D dopant profile is imaged due to selectively implanted phosphorous. Since the sample was annealed at 900 °C for 30 min, lateral straggle made the dopant smear into under the oxide mask, so that the capacitance image did not have a squarelike form but a circlelike form. The deformed shape can also be due to the shadowing effect as described earlier. The cross section of doping-dependent capacitance was seen in Fig. 4(c) which resembles recent results by Huang and co-workers.<sup>10</sup> The contour plot shown in Fig. 4(c) can be compared with a simulation result, which is in progress.

#### IV. SUMMARY

In summary, combined AFM and SCM was used to measure the local oxide thickness and dopant profile. The capaci-

tance for native oxide was measured revealing 2D dopant profile, and the effect of lateral diffusion and shadowing was demonstrated.

#### ACKNOWLEDGMENT

This work was partially supported by Samsung Electronics. Co., Ltd.

- <sup>1</sup>C. C. Williams, J. Slinkman, W. P. Hough, and H. K. Wickramasinghe, *Appl. Phys. Lett.* **55**, 1662 (1989).
- <sup>2</sup>C. C. Williams, J. Slinkman, W. P. Hough, and H. K. Wickramasinghe, *J. Vac. Sci. Technol. A* **8**, 895 (1990).
- <sup>3</sup>Y. Huang and C. C. Williams, *J. Vac. Sci. Technol. B* **12**, 369 (1994).
- <sup>4</sup>See, for example, E. H. Nicollian and J. R. Brews, *MOS Physics and Technology* (Wiley, New York, 1982).
- <sup>5</sup>G. Meyer and N. M. Amer, *Appl. Phys. Lett.* **53**, 1045 (1988).
- <sup>6</sup>S. Alexander, L. Hellemans, O. Marti, J. Schneir, V. Elings, P. K. Hansma, M. Longmire, and J. Gurley, *J. Appl. Phys.* **65**, 164 (1989).
- <sup>7</sup>J. R. Matey and J. Blanc, *J. Appl. Phys.* **47**, 1437 (1985).
- <sup>8</sup>C. C. Williams, W. P. Hough, and S. A. Rishton, *Appl. Phys. Lett.* **55**, 203 (1989).
- <sup>9</sup>O. Wolter, T. Bayer, and J. Greschner, *J. Vac. Sci. Technol. B* **9**, 1353 (1991).
- <sup>10</sup>Y. Huang, C. C. Williams, and J. Slinkman, *Appl. Phys. Lett.* **66**, 344 (1995).